Pergamon

Int. J. Heat Mass Transfer. Vol. 41, No. 13, pp. 1969–1981, 1998

Printed in Great Britain
0017-9310/98 $19.00+0.00

PII: S0017-9310(97)00288-3

Three-dimensional laser heating including evaporation—a kinetic theory approach

B. S. YILBAS† and M. SAMI

Mechanical Engineering Department, King Fahd University of Petroleum and Minerals, Dhahran, Saudi Arabia

(*Received* 17 *March* 1997 *and in final form* 19 *September* 1997)

Abstract—In laser heating process, energy is transmitted to the lattice site molecules through successive collisions. It is this collision mechanism, which describes the heating model. The present study is carried out to develop 3-D laser heating model including the phase change process. The probability of electron and lattice site atom collisions is considered in the case of conduction heating process while the probability of vacancy and molecular collisions is taken into account when dealing with the phase change process. Consequently, the collision probability of each species is considered when describing the conduction, melting and evaporation processes in laser pulse heating. Since the energy equation resulted is in the form of integro-differential equation, a numerical scheme is introduced to solve the governing equation. The temperature profiles predicted from the present study are, then, compared to the results obtained from the previous study. It is found that 3-D model gives lower surface temperatures as compared to the previous results obtained from 1-D model.

INTRODUCTION

Advancement in laser material processing in industry encourages the development of several model calculations of both spatial and temporal temperature profiles in laser heated solids. The surface treatment of engineering metals by laser heating becomes one of the important research fields in recent years [1–3]. Square-shaped temperature distribution induced by a Gaussian-shaped laser beam was predicted by Lu [4] using a Poisson equation with appropriate boundary conditions. Diniz Neto and Lima [5] developed non-linear 3-D heating model relevant to short pulse laser heating process. The governing equation of energy was solved numerically and the resulting temperature distributions were computed. However, the laser heating process was examined analytically by Yilbas [6] employing the intensity time dependent pulses. The equation of heat conduction was solved in the Laplace domain and the inversion was carried out using the Dawson's integral method. He showed that thermal integration of pulse heating was possible when the repetition rate of the heating pulse increased to 1 kHz. Laser heating process including the phase change was also investigated by several researchers [7–9]. Schulz *et al.* [10] examined heat conduction losses in laser cutting process. They solved the Fourier heat conduction equation through an analytical approximation. They showed that the power loss into substance through conduction was substantial and their results agreed well with the experimental findings. Moreover, analysis of heat conduction in deep penetration welding with a time-modulated laser beam was introduced by Simon *et al.* [11]. Steady state solution of governing energy equation based on Fourier heating was obtained analytically. The results indicated that the heat affected zone was not influenced by the temperature oscillations. Malian [3] introduced the solution of Poisson equation for the dual-beam CO_2 laser cutting process. He showed that theoretical predictions were in agreement with the experimental results. However, Yilbas and Sahin [12] introduced analytical solution to laser heating including the evaporation process. The solution was limited to step-input intensity and quasi-steady solution was attempted due to complicated nature of the process. Yilbas [13] introduced a numerical solution to laser heating appropriate to the laser drilling process. He employed 3-D heating model and vapor ejection was introduced through momentum equations. He showed that the prediction for the temperature rise well agreed with the experimental findings.

In the analysis of the laser matchining mechanisms which have been carried out to date the central feature, in general, has been the use of the Fourier conduction equation to describe the way in which photon energy from the laser beam is transferred to the atomic lattice of the workpiece material. It is this energy transfer mechanism which defines the laser interaction process and therefore the rate at which the material is removed through the evaporation. The Fourier equation of conduction for laser heating of solids is not strictly valid, due to the assumptions made in the theory. The heat flux through a given plane depends on the electron distribution through the substance. On the scale distance required to examine the conduction pro-

† Author to whom correspondence should be addressed.

NOMENCLATURE

dt	time increment [s]
dx	spatial increment [m]
C_p	specific heat [J (kg·K)$^{-1}$]
$E_{s,t}$	electron energy [J]
$E_{x,t}$	phonon energy [J]
f, g, h	fraction of excess energy exchange
I_0^1	laser peak power intensity [W m^{-2}]
k	thermal conductivity [W (m·K)$^{-1}$]
k_B	Boltzmann's constant [1.38×10^{-23} J K^{-1}]
M, m	molecular mass or mass flux [kg]
N	electron number density [l m^{-3}]
N_0	number density of lattice site [l m^{-3}]
P_{bm}	probability of bound molecule collision
P_{fm}	probability of free molecule collision
P_h	probability of vacancy
$T(s, y, z, t)$	electron temperature in the x-axis
$T(x, \eta, z, t)$	electron temperature in the y-axis
$T(x, y, \xi, t)$	electron temperature in the z-axis
U	potential energy [J]
$\bar{V}$	electron mean velocity [m s^{-1}].

Greek symbols

α	thermal diffusivity [m^2 s^{-1}]
λ	mean free path of electrons [m]
δ	absorption coefficient [l m^{-1}]
μ	mean free path of molecules [m]
ρ	density [kg m^{-3}].

cess, the material can no longer be considered as being a continuum. When the machining power intensities ($\sim 10^{11}$ W m^{-2}) are concerned the higher-order terms in the heat transfer equation become important [14]. Consequently, the heating mechanism appropriate to laser machining process should be examined on a microscopic level and the development of a new model describing the process becomes necessary.

The limitations in the application of Fourier heating model is laser material processing led to the development of a new heating model relevant to pulsed laser machining process. The model involved essentially an energy transfer mechanism, which occurred during successive collisions of electrons with lattice atoms [15]. In this case; the free electron gains energy from the laser beam via absorption and makes successive collisions with the lattice atoms. It is this collision process which defines the energy conduction mechanism. Qin and Tien [16] introduced an electron–lattice atom collision process when modeling two-step heat conduction model. However, the model developed was based on Fourier heat conduction equation and the electron–phonon collision was incorporated through a coupling factor. Yilbas [17], developed the heating model, based on electron-kinetic theory approach, allowing the evaporation process. The study was limited to 1-D heating process. On the other hand, the motion of the electrons in the vicinity of the surface is free and 3-D. Consequently, 3-D heating model should be considered for improved accuracy. In the present study, 3-D laser heating model is developed using an electron-kinetic theory approach. Evaporation process is also taken into account and the numerical solution is attempted with appropriate boundary conditions. In addition, the surface temperature profiles predicted are, then, compared to previous finding [17].

MODELING OF HEATING PROCESS

The electron kinetic theory approach in laser heating process relies on the electron–photon interactions. In this case, laser beam energy interacts with the workpiece electrons in the conduction band in the form of photons. Absorption of the photon energy by the electrons leads successive collisions between the excited electrons and lattice phonons, which in turn excite the lattice phonons to higher energies. Once the phonon energy increases, phonon–phonon collisions take place in such a way that the collisions tend to restore the thermal equilibrium.

The mathematical formulation of the heating mechanism may be distinguished into two groups. These include heat conduction only process (conduction limited heating) and heat conduction and phase change processes (non-conduction limited heating). However, before formulating each process, some useful assumptions need to be introduced. Steady state space change is assumed, in which exactly the same number of electrons are emitted from the material as are returning from the space charge, therefore, energy losses due to thermionic emission is neglected. Local equilibrium is assumed before the initiation of heating (at $t = 0$). The mean free path of electrons is independent of temperature and electron–electron collisions are assumed to be elastic. Finally, it is also assumed that the solid is free from impurities.

The electron motion and relevant collision processes are modeled using a cartesian coordinate system. The mathematical model governing the heating process and based on the above assumptions are given under the following sub-headings.

Conduction limited heating

The electron motion in solid substance close to free surface is shown in Fig. 1. The atom is fixed in a lattice

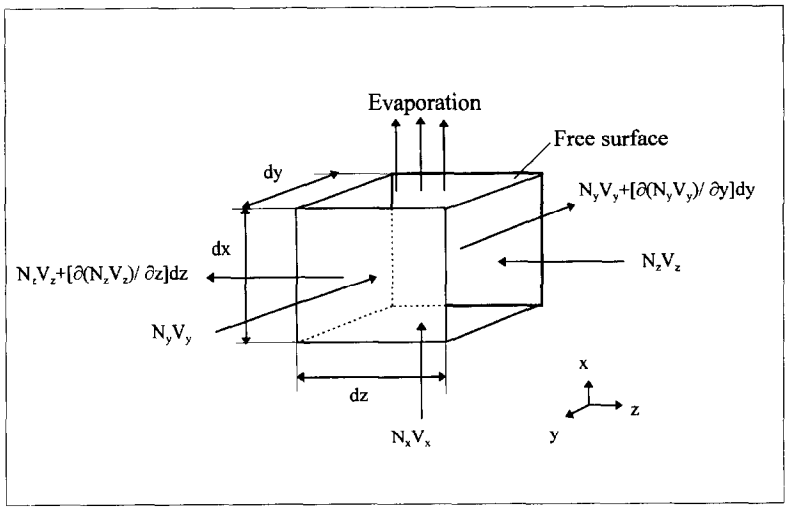

Fig. 1. 3-D view of control volume.

site in solid state and its thermal energy is manifested as vibrations of atom above the equilibrium position [18]. When an atom vibrates, the periodic field of lattice is continuously perturbed. Since the velocity with which the atoms vibrate is much smaller than the velocity of the free electrons, the atom may be assumed to lie at its displaced position. Consequently, in considering bound atom–electron collision process, the bound atom may be situated at its displaced position and will have a vibrational energy at this position of:

$$E = \frac{h\omega}{\exp\left(\frac{h\omega}{k_B T}\right) - 1}$$

which for $h\omega = k\theta_E$, where θ_E is the characteristic Einstein temperature and $T \gg \theta_E$ yields:

$$E = k_B T.$$

Energy increase of atom, due to electron–atom collision, manifest itself as an increase in the amplitude of the phonon vibration, which in turn forces the neighboring atoms to new equilibrium positions. Some energy, however, is also absorbed by the neighboring atoms through damping the energy increase of the heat collided atom. A stage is reached where eventually the atoms in the region of the original collision site are all in equilibrium and increased vibrational energies, i.e. increased thermal energies.

In accordance with Fig. 1, the number of electrons having the average velocity $\bar{V}_x$ entering the control volume in the x-axis through area $dy\,dz$ at time dt is:

$$N_x \bar{V}_x\,dy\,dz\,dt \quad \text{where } dy\,dz = A_x.$$

The probability of electron traveling a distance x, where $x \ll 2\lambda$ (λ being the mean free path), without making a collision is:

$$\frac{dx}{\lambda}.$$

However, the arguments relevant to collision probability is not given here due to lengthy arguments, but refer to [14]. Therefore, the total collision probability of the electrons moving in x-direction can be written as:

$$\int_{-\infty}^{\infty} N_x \bar{V}_x A_x \exp\left(-\frac{(x-s)}{\lambda}\right)\frac{ds}{\lambda}\frac{dx}{\lambda}.$$

The negative bound of the integral is due to minor image introduced at the free surface of the workpiece for the reflected electrons [15]. The net transfer of energy during the electron phonon collision throughout the material in the x-axis is:

$$\Delta E_{x,t}\int_{-\infty}^{\infty} N_x \bar{V}_x A_x \exp\left(-\frac{(x-s)}{\lambda}\frac{ds}{\lambda}\frac{dx}{\lambda}\right)(E_{s,t}-E_{x,t})$$

where $E_{s,t}$ is the electron energy and $E_{x,t}$ is the phonon energy in the x-axis.

In a similar manner, the probability of total electron–phonon collision throughout the material in the y-axis can be written as:

$$\int_{-\infty}^{\infty} N_y \bar{V}_y A_y \exp\left(-\frac{|x-\eta|}{\lambda}\right)\frac{d\eta}{\lambda}\frac{dx}{\lambda}.$$

The lower bound of the integral is set to $-\infty$. Although no-free surface is available in the y-axis, the source of electrons extends to both directions of the y-axis from the control element.

The transfer of energy in the y-axis during the collision process is:

$$\Delta E_{y,t}\int_{-\infty}^{\infty} N_y \bar{V}_y A_y \exp\left(-\frac{|y-\lambda|}{\lambda}\right)\frac{d\eta}{\lambda}\frac{dy}{\lambda}(E_{\eta,t}-E_{y,t})$$

where $E_{\eta,t}$ is the electron energy and $E_{y,t}$ is the phonon energy in the y-axis.

Similarly, the energy transfer taking place in the z-axis during the collision process is:

$$\Delta E_{z,t}\int_{-\infty}^{\infty} N_z \bar{V}_z A_z \exp\left(-\frac{|z-\xi|}{\lambda}\right)\frac{d\xi}{\lambda}\frac{dz}{\lambda}[E_{\xi,t}-E_{z,t}]$$

where $E_{\eta,t}$ is the electron energy and $E_{z,t}$ is the phonon energy in the z-axis.

Energy increased per unit volume in the substance due to area A_x and in increment dx during the time interval dt is:

$$\frac{\Delta E_{x,t}}{A_x\,dx\,dt}.$$

In a similar fashion, energy increase per unit volume in the substance across the areas A_y and A_z and in increments dy and dz during time interval dt are:

$$\frac{\Delta E_{y,t}}{A_y\,dy\,dt} \quad \text{and} \quad \frac{\Delta E_{z,t}}{A_x\,dz\,dt}$$

respectively.

However, it is assumed that the process of absorption of laser beam occurs by absorption of photons by electrons. The process can be described by Lambert's law. In fact, quantum mechanical analysis shows that photons may be absorbed both by the free electrons and by the bound electrons in the atomic shells. This process can only occur with the transfer of discrete quanta of energy. However, in order to maintain the simplicity of the present model, these quantum effects can be ignored and the electrons are assumed to require merely by passing through the electromagnetic field of the incident laser beam in a manner described by Lambert's law.

The total amount of energy which is absorbed in a depth with area A in time dt due to laser irradiation is:

$$I_0 A\,dA\,d\Psi\cdot f'(\Psi)\cdot\frac{N_{sx}}{N_{sx}+N_{xs}}.$$

It is possible that electron density may vary through the material and, in particular, the number of electrons travelling from ds to dx (Fig. 2) may not be the same as that from dx to ds. Therefore, the proportion of energy which is absorbed by the electrons which travel from ds to dx in time dt is:

$$I_0\cdot A\cdot dt A\,d\Psi\cdot f'(\Psi)\cdot\frac{N_{sx}}{N_{sx}+N_{xs}}$$

where $f'(\Psi)$ is the absorption function, which is:

$$f'(\Psi) = -\frac{d}{d\psi}[\exp(-\delta|\psi|)]$$

and N_{xs} is the number of electrons travelling from dx to ds. The average energy absorbed by the electrons in $d\psi$ is:

$$\Delta E\,|_{\text{abs}} = I_0\cdot A\cdot dt\cdot\int_x^s \frac{N_{sx}f'(\Psi)\,d\Psi}{(N_{sx}+N_{xs})}.$$

However, a spatial distribution of the power intensity at the surface may be assumed Gaussian, i.e.:

$$\Delta E\,|_{\text{abs}} = \frac{I_0^l}{2\sqrt{\pi a}}\exp\left(-\frac{y^2+z^2}{a^2}\right)\cdot A \cdot dt\int_x^s \frac{N_{sx}}{(N_{sx}+N_{xs})}\cdot f'(\psi)\,d\psi.$$

Consequently, the energy absorbed by the substance per unit volume and unit time becomes:

$$\Delta E\,|_{\text{abs}} = \frac{\Delta E\,|_{\text{abs}}}{A_x\cdot d_x\cdot dt}$$

or

$$\Delta E\,|_{\text{abs}} = \frac{I_0^l}{2\sqrt{\pi a}}\exp\left(-\frac{y^2+z^2}{a^2}\right)\frac{d}{dx} \times\int_x^s \frac{N_{sx}}{(N_{sx}+N_{xs})}\cdot f'(\psi)\,d\psi.$$

Therefore, total energy increase per unit volume is related to internal energy gain of the substance, i.e.:

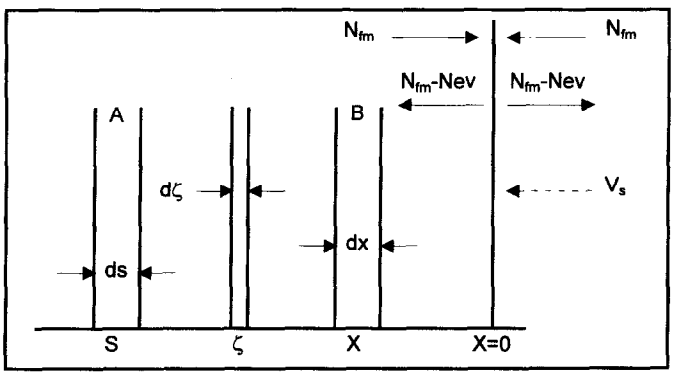

Fig. 2. Electron movement in the surface region ($x = 0$ is the free surface).

$$\frac{\Delta E_{x,t}}{A_x\,\mathrm{d}x\,\mathrm{d}t}+\frac{\Delta E_{y,t}}{A_y\,\mathrm{d}y\,\mathrm{d}t}+\frac{\Delta E_{z,t}}{A_z\,\mathrm{d}z\,\mathrm{d}t}+\frac{\Delta E\,|_{\text{abs}}}{A_x\,\mathrm{d}x\,\mathrm{d}t}=\frac{\mathrm{d}}{\mathrm{d}t}[\rho C_p T(x,y,z,t)].$$

It should be noted that

$$A_x=\mathrm{d}y\,\mathrm{d}z,\quad A_y=\mathrm{d}x\,\mathrm{d}z\quad\text{and}\quad A_z=\mathrm{d}x\,\mathrm{d}y.$$

Furthermore, assuming that the thermal properties are independent of temperature. The total energy equation yields:

$$\rho C_p\frac{\mathrm{d}}{\mathrm{d}t}T(x,y,z,t)=\int_{-\infty}^{\infty}\frac{N_x\bar{V}_x A_x}{\lambda^2}\times\exp\left(-\frac{|x-s|}{\lambda}\right)\mathrm{d}s\,\mathrm{d}x[E_{s,t}-E_{x,t}]+\int_{-\infty}^{\infty}\frac{N_y\bar{V}_y A_y}{\lambda^2}\exp\left(-\frac{|y-\eta|}{\lambda}\right)\mathrm{d}\eta\,\mathrm{d}y[E_{\eta,t}-E_{y,t}]+\int_{-\infty}^{\infty}\frac{N_z\bar{V}_z A_z}{\lambda^2}\exp\left(-\frac{|z-\xi|}{\lambda}\right)\mathrm{d}\xi\,\mathrm{d}z[E_{\xi,t}-E_{z,t}]+\frac{I_0^1}{\sqrt{2\pi a}}\exp\left(-\frac{y^2+z^2}{\alpha^2}\right)\frac{\mathrm{d}}{\mathrm{d}x}\times\int_x^s\left(\frac{N_{sx}}{N_{sx}+N_{xs}}\right)\cdot f'(\psi)\cdot\mathrm{d}\psi.$$

It should be noted that

$$E_{s,t}=k_B T(s,y,z,t);\quad E_{\eta,t}=k_B T(x,\eta,z,t)\quad\text{and}\quad E_{\xi,t}=k_B T(x,y,\xi,t)$$

introducing a fraction 'f' for the energy transfer and explicit formulation of the total energy equation may be written as:

$$T(x,y,z,t+\mathrm{d}t)=\left[\frac{I_0^1}{2\sqrt{\pi a}}\exp\left(-\frac{y^2+z^2}{a^2}\right)\times\frac{\mathrm{d}}{\mathrm{d}x}\left[\int_x^s\frac{N_{sx}}{N_{sx}+N_{xs}}\cdot f'(\psi)\cdot\mathrm{d}\psi\right]+\frac{fk}{4\lambda^3}\frac{\Delta t}{\rho C_p}\left[\int_0^{\infty}\exp\left(-\frac{|x+s|}{\lambda}\right)T(s,y,z,t)\,\mathrm{d}s+\int_0^x\exp\left(-\frac{|x-s|}{\lambda}\right)T(s,y,z,t)\,\mathrm{d}s+\int_0^x\exp\left(-\frac{|x-s|}{\lambda}\right)T(s,y,z,t)\,\mathrm{d}s\right]+\frac{fk}{2\lambda^3}\frac{\Delta t}{\rho C_p}\left[\int_0^{\infty}\exp\left(-\frac{|y-\eta|}{\lambda}\right)T(x,\eta,z,t)\,\mathrm{d}\eta\right]+\frac{fk}{2\lambda^3}\frac{\Delta t}{\rho C_p}\left[\int_0^{\infty}\exp\left(-\frac{|z-\xi|}{\lambda}\right)T(x,y,\xi,t)\,\mathrm{d}\xi\right]+T(x,y,z,t)\left[1-\frac{3f\alpha\,\mathrm{d}t}{2\lambda^2}\right]\quad(1)$$

where k is the thermal conductivity [$k=(N/3)/k_B\bar{V}\lambda$] and α is the thermal diffusivity [$\alpha=(k/\rho C_p)$].

The details of the arrangement of total energy equation and fraction 'f' are given in [15].

However, the equation governing the relation between the molecules was developed using standard scattering rate equations, in which electron–phonon coupling parameters were introduced [19]. In this case the resulting equations may be written as:

In the x-axis:

$$T(s,y,z,t)\frac{\partial T(s,y,z,t)}{\partial t}=-\frac{3h}{\pi k_B}\lambda(w^2)[T(s,y,z,t)-T(x,y,z,t)].$$

In the y-axis:

$$T(x,\eta,z,t)\frac{\partial T(x,\eta,z,t)}{\partial t}=-\frac{3h}{\pi k_B}\lambda(w^2)[T(x,\eta,z,t)-T(x,y,z,t)].$$

In the z-axis:

$$T(x,y,\xi,t)\frac{\partial T(x,y,\xi,t)}{\partial t}=-\frac{3h}{\pi k_B}\lambda(w^2)[T(x,y,\xi,t)-T(x,y,z,t)]\quad(2)$$

where w^2 is the second moment of the phonon spectrum, k_B is the Boltzmann's constant and λ is the electron–phonon coupling parameter.

To obtain a temperature field, relevant to heating process, for lattice sites and electrons, equations (1) and (2) should be solved simultaneously.

Non-conduction limited case

The evaporation process relevant to non-conduction limited heating may be explained in the following manner. In releasing the molecule from the lattice, a vacancy is left behind. This vacancy can be filled by other free molecules but in the process energy is released. The molecule released from the lattice is immediately captured in a new equilibrium position, i.e. either in a vacant hole or in an interstice. When a molecule leaves the lattice and fixes itself in an interstitial position, the dissociation process is not completed, since the molecule can easily return. It is only when either the molecule leaves this site for another interstice or vacancy, or the vacancy moves to another site by being filled with another molecule, that the dissociation process is completed. In this way a vacancy is created in the lattice. However, vacancies can also be adsorbed from the surface, as interstitial atoms. In the first case a surface atom may move

from its equilibrium position outwards, as in normal evaporation. However, instead of escaping, it is recaptured at a new position on top of the existing surface layer. As a result a vacancy is formed at the original lattice site which is quickly filled by a molecule from the next row. In this way vacancy is adsorbed into the material and can then move freely around the interior lattice. It should be noted that evaporation process (free molecular motion) takes place in 1-D that is from the free surface. In this case free molecular motion is considered as 1-D and in the axis perpendicular to the surface, i.e. the x-axis motion only. The volumetric evaporation may be summarized as that the interior process is 3-D, but it is modified at the free surface by the fact that molecules may escape in 1-D. The method of analysis considers the workpiece as an infinite block of material. Moreover, the surface is moving at a velocity V_s in the x-axis and molecules are escaping from the surface. Therefore, a net mass flux through the surface of evaporating molecules occurs. The assumption is made that this net flow is reflected through out the material, an assumption which corresponds to neglecting the effects of shock waves. In this case, the coordinate axes are moving with a velocity V_s and therefore all mass transport processes involve relative velocities.

The average velocity with which the free molecules move about in the lattice may be written as:

$$V_f = V_{th} \exp\left[-\frac{U}{k_B T}\right]$$

where U and V_{th} are the energy required to form a free molecule and thermal velocity, respectively. The details of the analysis of molecular movement is not given here due to length arguments, but refer to [17].

The number of free molecules per unit volume throughout the material at temperature T is:

$$N_{fm} = N_0 \exp\left[-\frac{U_1}{k_B T}\right]$$

and the number of vacancies per unit volume is:

$$N_h = N_0 \exp\left[-\frac{U_2}{k_B T}\right]$$

where $U_{1,2}$ are the activation energy and N_0 is the number of lattice sites per unit volume. It is also evident that

$$N_{bm} + N_h = N_0$$

where N_{bm} is the number of density of bound molecules.

When considering the molecular energy transfer from the surface region (Fig. 2) through molecular movement, the energy equation including the evaporation process may be resulted. The details of derivation of the energy equation are given in [17]. Consequently, the resulting energy equation is:

$$\frac{\partial T(x,y,z,t)}{\partial t} = \frac{I_0^1 \delta}{2\sqrt{\pi a \rho C_p}} \times \exp\left[-\frac{y^2+z^2}{a^2}\right] \cdot \int_x^s \frac{N_{xx}}{N_{xx}+N_{xs}} \cdot f'(\psi)\, d\psi - \left[\frac{3fk}{2\lambda^2 \rho C_p} + \frac{k}{2\mu^2 \rho C_p}(p_{fm}h + p_{bm}g + 2p_h)\right] + \frac{fk}{4\lambda^3 \rho C_p}\left[\int_0^\infty \exp\left(-\frac{|x+s|}{\lambda}\right) \cdot T(s,y,z,t)\, ds + \int_0^x \exp\left(-\frac{|x+s|}{\lambda}\right) \cdot T(s,y,z,t)\, ds + \int_0^\infty \exp\left(-\frac{|x+s|}{\lambda}\right) \cdot T(s,y,z,t)\, ds\right] + \frac{fk}{2\lambda^3 \rho C_p}\left[\int_0^\infty \exp\left(-\frac{|y-\eta|}{\lambda}\right) \cdot T(x,\eta,z,t)\, dy\right] + \frac{fk}{2\lambda^3}\frac{\Delta t}{\rho C_p}\left[\int_0^\infty \exp\left(-\frac{|z-\xi|}{\lambda}\right) T(x,y,\xi,t)\, d\xi\right] + \frac{k}{\rho C_p}\int_{-\infty}^\infty \frac{P_{fm} \cdot h}{2\mu^2} \exp\left(-\frac{|x-s|}{\mu}\right) T(s,y,z,t)\, ds + \frac{k}{\rho C_p}\int_{-\infty}^\infty \frac{p_{bm} \cdot g}{2\mu^2} \exp\left(-\frac{|x-s|}{\mu}\right) T(s,y,z,t)\, ds + \frac{k}{\rho C_p}\int_{-\infty}^\infty \frac{p_h}{2\mu^2} \exp\left(-\frac{|x-s|}{\mu}\right) \times [U(s) - U(x) + 3k_B T(s,y,z,t)\, ds\Bigg]. \quad (3)$$

It is evident that equation (3) has two parts including conduction and phase change processes. The conduction part of the equation is identical to equation (1), therefore, when solving the conduction part, equation (2) should be taken into account, i.e. conduction part and equation (2) should be solved simultaneously to obtain electron and lattice site atom temperatures.

NUMERICAL SOLUTION TO PULSE HEATING

The energy equations governing both conduction and non-conduction limited heating processes are in the form of integro-differential equations, which do not yield analytical solutions. Therefore numerical scheme should be introduced. An explicit method is introduced to discritize the governing equations providing that it requires to meet a stability criterion for a convergent solution. The discritization procedure is not given here due to length arguments, but refer to [17]. In the case of conduction limited heating, the stability criterion is:

$$\frac{3fd\Delta t}{2\lambda^2} \leqslant 1.$$

The calculated time increment meeting the stability criterion is 10^{-10} s and this value is used in computation. On the other hand, the discritization procedure for non-conduction limited heating is given in the appendix. The stability requirements for this case is:

$$\left[\frac{3fk\Delta t}{2\lambda^2\rho C_p} + \frac{p_{fm}\cdot h\cdot k\cdot \Delta t}{2\mu^2\rho C_p} + \frac{p_{bm}\cdot g\cdot k\cdot \Delta t}{2\mu^2\rho C_p} + \frac{2p_h\cdot k\cdot \Delta t}{2\mu^2\rho C_p}\right] \leqslant 1.$$

The time increment meeting the stability criterion is 10^{-12} s and it is this time increment, which is used in computation.

In order to compare the present predictions with the previous results, the pulse shaped used in the previous study is employed in computing the temperature profiles in the present study. The pulse profile used in the present study is shown in Fig. 3. It should be noted that the pulse profile used in the present study resembles the actual pulse profile used in the previous study.

The material selected in the present study is stainless steel and the ambient gas effect during laser heating process is omitted by assuming inert gas environment.

RESULTS AND DISCUSSIONS

3-D laser pulse heating process is successfully modeled using an electron-kinetic theory approach. Conduction and non-conduction limited cases are introduced and the respective governing equations are solved numerically.

Figure 4 shows 3-D temperature profiles inside the substance while Fig. 5 shows the temperature distribution inside the substance at different heating times. As the heating time progresses, rapid decrease in temperature occurs in the vicinity of the surface. In this case, electron energy gain, due to laser radiation, becomes considerably high in the vicinity of the surface. Consequently, energy transfer to the lattice site atoms is considerable during electron–atom collision; i.e. phonon energy in the vicinity of the surface increases substantially. Moreover, the phonon-relaxation process is relatively slower as compared to electron relaxation. Therefore, the rate of thermal conduction to the solid substance becomes less than the internal energy gain of the substance in the vicinity of the surface due to collisional processes. However, as the distance from the surface increases the energy of the excited electrons reduces due to one or both of the following reasons: (i) excited electrons loses their excess energy when colliding with the atoms in the surface vicinity, therefore, less energetic electrons may reach to this region and (ii) the time at which the energy conducted through the collisional process into this region progresses, which in turn results in more energy transfer to the atoms situated into this region, through phonon relaxation process. As the temperature reaches to the melting temperature, energy needed to form unbounded molecules (liquid molecules) becomes significant and energy gain from the external field balances the losses due to heat conduction and formation of liquid molecules. Consequently, the temperature of the substance remains almost constant at certain depths. However, as depth inside the substance increases further, the energy balance can no longer be sustained due to absorption of incident beam which does not extend up to this region, consequently conduction losses dominate and melting ceases, i.e. temperature of the substance drops below the melting temperature. On the other hand when the temperature reaches the evaporation temperature, molecules evaporate and leave vacancies behind. The vacancies can be replaced by the molecules behind. Consequently, probabilities of the vacancy–bond molecule and free molecule–vacancy collisions become important. In this case, evaporating molecules take energy from the surface resulting energy losses at the surface. The energy gain due to absorption of incident laser beam is substantial at the surface. Therefore, the temperature of the surface rises at a relatively slow rate as compared to no-evaporation case. It is also evident from Fig. 5 that the rate of temperature rise in the substance just before the evaporation (at time 0.3 μs) is less than that corresponds to the after evaporation process (at time 0.6 μs). This may indicate that once the melting initiates the energy consumed by heating the liquid becomes substantial, in addition to this, energy required for the propagation of the melt isotherms into the solid substance is considerable. Therefore, the rate of internal energy gain, due to laser radiation, reduces in the vicinity of the free surface.

Figure 6 shows the 3-D temperature distribution across the irradiated spot while Fig. 7 shows the temperature distribution at different heating times. The temperature distribution along the y-axis is very smooth before the melting temperature is reached ($t = 0.1$ μs). Once the melting results, the temperature remains constant at some distance away from the heated spot center. In this case, the probability of forming the melt molecules is considerable and the energy gain by the external field is balanced by the conduction and phase change processes as discussed earlier. As the heating time progresses, the melt temperature increases substantially in the region of 10 μm of the irradiated spot. When the evaporation process initiates, energy required to form the free molecules increases, which in turn results almost constant temperature at the surface ($t = 0.6$ μs). The rate of decay of temperature corresponding to 0.6 μs heating time is very small along the distance 2.6–7 μm, on the other hand, rapid temperature increase is resulted in the vicinity of the center of the heated spot. This indicates that the internal energy of the substance in the surface region increases, therefore, the probability of the for-

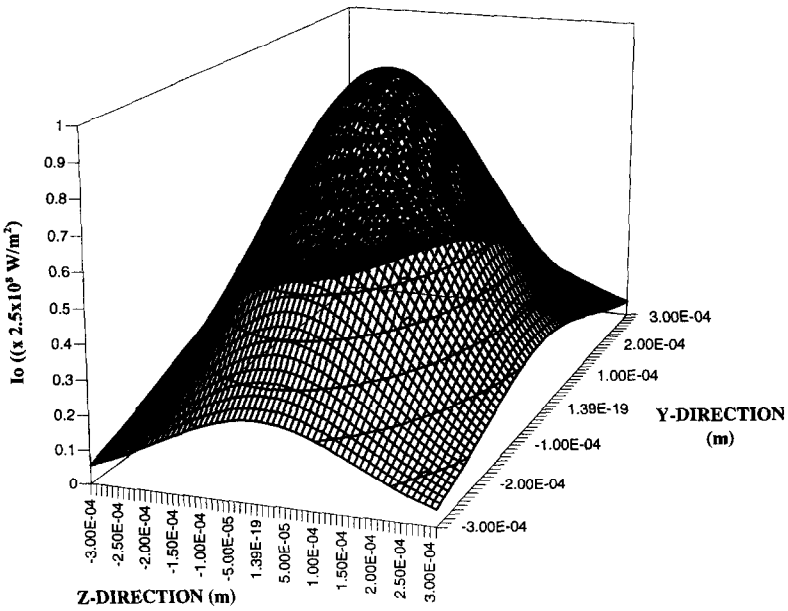

Spatial distribution of laser output pulse.

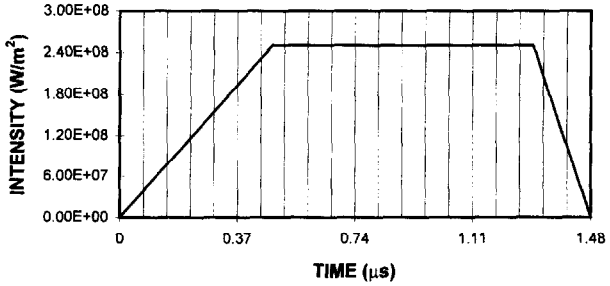

Temporal variation of laser output pulse.

Fig. 3. Laser pulse profile used in the computation.

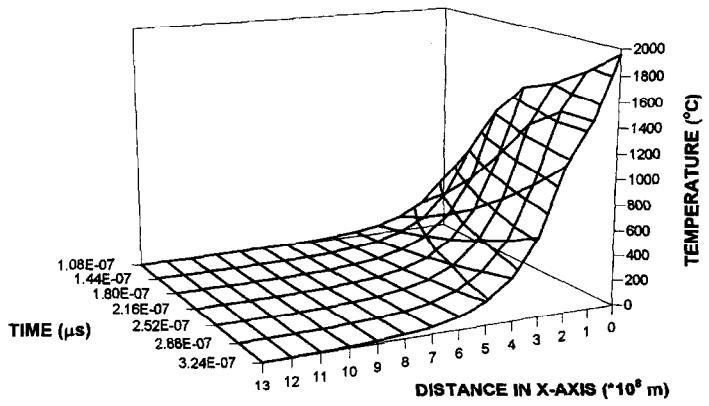

Fig. 4. 3-D temperature profiles inside the substance.

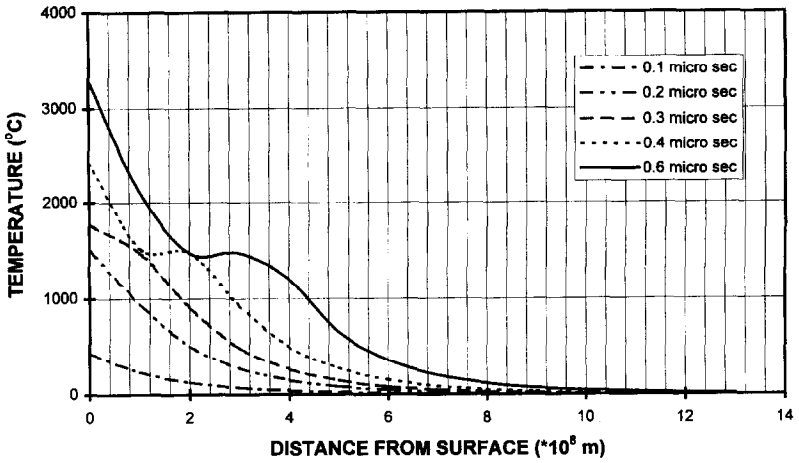

Fig. 5. Temperature profiles inside the substance at different heating times.

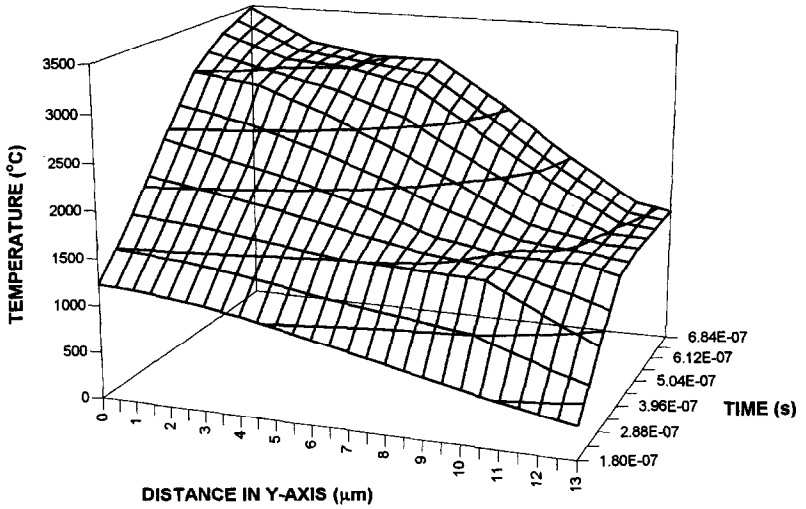

Fig. 6. 3-D temperature distribution across the heated spot.

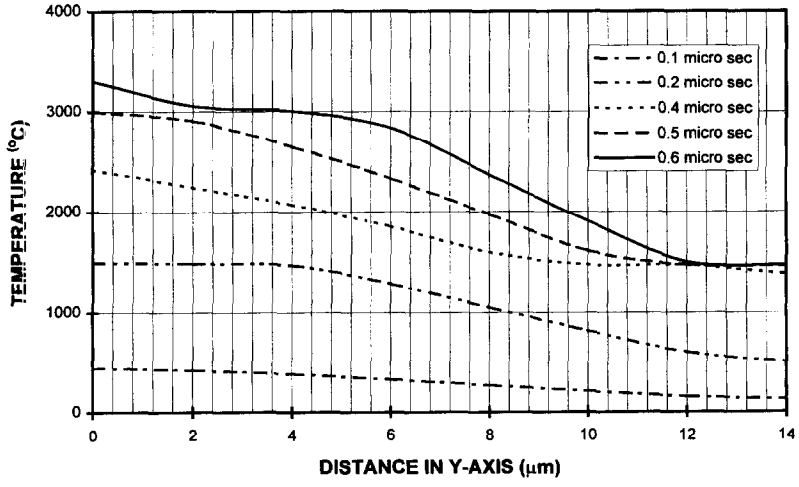

Fig. 7. Surface temperature profiles along y-axis at different heating times.

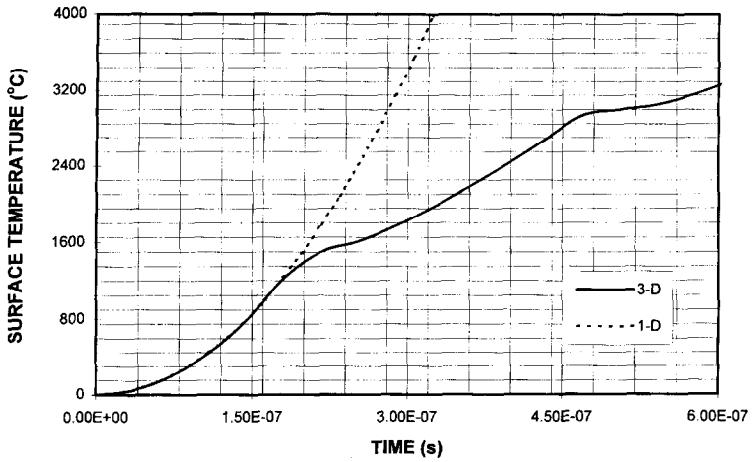

Fig. 8. Temporal variation of surface temperature obtained from both 1-D and 3-D heating models.

mation of evaporating molecules is not sufficiently high causing substantial convective energy loss from the surface.

Figure 8 shows the surface temperature rise at the center of the heated spot obtained from the present and previous studies [17]. Both temperature profiles almost coincides during the conduction limited heating phase of the process. Once the heating progresses, the temperature corresponding to 3-D model becomes lower than that correspond to 1-D heating model developed previously [17]. In this case, heat transfer in radial direction plays an important role. The electron-collision takes place in all directions, and electron energy reduces further through successive collisions while the phonon energy in the radial direction increases. Therefore, the temperature at the center of the irradiated spot becomes less as compared to one-dimensional heating process. As it is indicated before, immediately after the initiation of the melting process the rate of surface temperature rise reduces and the probability of the formation of liquid molecules increases, which in turn results in relatively slow rate of internal energy gain as compared to the case occurring in the conduction limited heating. As the heating progresses beyond the point of evaporation, the rate of internal energy gain further slows down and there appears to be an energy balance developing among the evaporating molecules, heat conduction losses and internal energy gain of the substance. The contribution of energy requirement to form the evaporating molecules on this energy balance is not substantial. However, the discrepancies between the results predicted from both 1- and 3-D models relevant to conduction limited heating are not considerable which may be due to the scale of heating process, i.e. the diameter of the incident beam at the free surface of the workpiece is 300 μm.

Figure 9 shows the temperature gradient (dT/dt) with dimensionless heating time ($\alpha\delta^2 t$). As the heating progresses three peaks (maximum points) in the curve is evident. These maximum points are due to change of slope of the curve, i.e. they indicate the initiation of phase change processes, except the first maxima. This may be due to the fact that in the pulse beginning, the internal energy gain is considerable due to absorption of laser radiation. As the heating time increases, the conduction of energy, through successive collisions of electron–phonon, increases. In this case, an energy balance may be attained, i.e. conduction losses balance the internal energy gain of the substance in the surface vicinity. At this point, an equilibrium time may be introduced, i.e. the equilibrium time may be defined as a time which energy losses balances the internal energy gain via absorption of a laser beam. However, a relation may exist among the equilibrium time, material properties and heating pulse shape. This relation may be written as:

$$t_{\text{equib}} = \text{const.}/\alpha\delta^2.$$

In this case, constant in the above relation may be related to pulse shape.

CONCLUSIONS

Temperature gradient (dT/dx) is substantial in the vicinity of the surface as heating progresses. In this case electron gains considerable energy via absorption of the incident beam and transfers their excess energy to the lattice atoms through successive collisions in the vicinity of the surface. The phonon relation process is relatively slow, therefore, the rate of energy dissipation (conducted) towards the bulk of the substance from the surface by phonon relaxation process is relatively smaller than the internal energy gain of the substance in the vicinity of the surface through successive electron–phonon collisions, i.e. substantial temperature gradient is resulted. As the heating progresses further, the rate of energy conducted, through

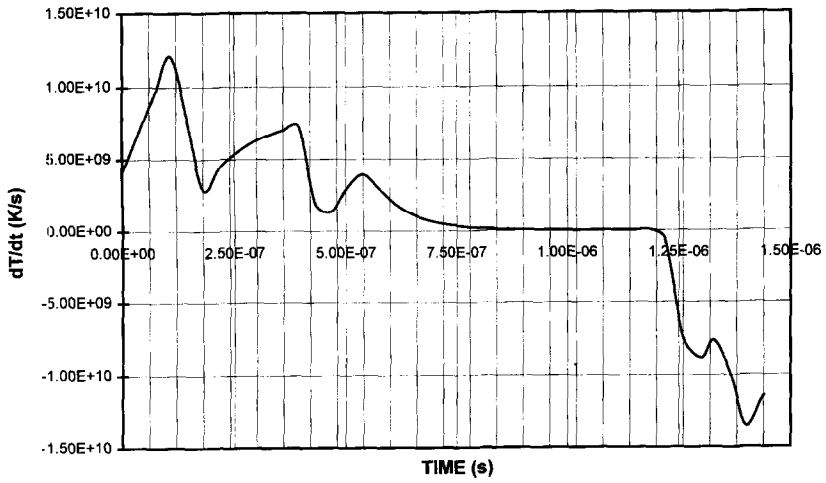

Fig. 9. Variation of dT/dt with time.

the collisional processes to the bulk of the solid substance increases.

When the temperature reaches to evaporation temperature, the energy required for the formation of free molecules becomes significant and internal energy increase, due to absorption of the incident beam, slows down. Therefore, an energy balance may occur among the absorbed energy, internal energy gain of the substance and latent heat of melting and evaporation. Consequently, energy gain from the external field may be dissipated significantly due to the formation of liquid and evaporating molecules. It should be noted that the propagation of melt isotherms results in less internal energy increase in the vicinity of the surface.

Surface temperature profile predicted from the present study for the conduction only process is almost similar to the temperature profile obtained from the previous study (1-D heating model). Once the phase change initiates, the surface temperature becomes less than that obtained from the previous study. This may be due to that in 3-D model, the electron–phonon collisions take place in all directions. The electron energy reduces further through successive collisions in radial direction, therefore, the internal energy gain due to absorption of incident beam reduces due to radial heat conduction. Moreover, immediately after the initiation of the melting process, the rate of surface temperature rise reduces and the probability of the formation of liquid molecules in all directions increase, which in turn results in relatively low surface temperatures as compared to the results of 1-D model. It is evident that once the evaporation occurs, the rate of increase of internal energy in the surface vicinity reduces further.

In the initial phase of the heating process, an equilibrium point may be attained, in this case; energy balance between the internal energy gain and the conduction losses at the surface may occur. It may appear that the equilibrium time may depend upon the heating pulse shape and the material properties.

REFERENCES

1. Zhong, H. J., Non-quasi steady analysis of heat conduction from a moving heat source. *Transactions of ASME, Journal of Heat Transfer*, 1990, **112,** 777–779.
2. Modest, M. F. and Abakians, H., Heat conduction in a moving semi-infinite solid subject to pulsed laser irradiation. *Transactions of ASME, Journal of Heat Transfer*, 1986, **108,** 597–601.
3. Malian, P. A., Dual beam CO_2 laser cutting of thick metallic materials. *Journal of Materials Science*, 1993, **28,** 1738–1748.
4. Lu, Y. F., Square-shaped temperature distribution induced by a Gaussian-shaped laser beam. *Applied Surface Science*, 1994, **81,** 357–364.
5. Diniz Neto, O. O. and Lima, C. A. S., Non-linear three dimensional temperature profiles in pulsed laser heated solids. *Journal of Physics D: Applied Physics*, 1994, **27,** 1795–1804.
6. Yilbas, B. S., Analytical solution for heat conduction mechanism appropriate to the laser heating process. *Int. Comm. Heat and Mass Transfer*, 1993, **20,** 545–555.
7. Yilbas, B. S. and Sahin, A. Z. and Davies, R., Laser heating mechanism including evaporation process initiating the laser drilling. *International Journal of Machine Tools and Manufacture*, 1995, **35**(7), 1047–1062.
8. Yilbas, B. S., Study into a numerical solution for a pulsed CO_2 heating process. *Numerical Heat Transfer, International Journal of Computation and Methodology, Part A—Applications*, 1995, **28**(4), 281–290.
9. Kaplan, A., A model of deep penetration laser welding based on calculation of the keyhole profile. *Journal of Physics D: Applied Physics*, 1994, **27,** 1805–1814.
10. Schulz, W., Beeker, D., Franke, J., Kemmerling, R. and Herriger, G., Heat conduction losses in laser cutting of metals. *Journal of Physics D: Applied Physics*, 1993, **26,** 1357–1363.
11. Simon, G., Grotzke, U. and Kross, J., Analysis of heat conduction in deep penetration welding with a time-modulated laser beam. *Journal of Physics D: Applied Physics*, 1993, **26,** 862–869.
12. Yilbas, B. S. and Sahin, A. Z., Laser heating mechanism including evaporation process. *Int. Comm. Heat and Mass Transfer*, 1994, **21**(4), 509–518.
13. Yilbas, B. S., Laser heating process and experimental validation. *International Journal of Heat and Mass Transfer*, 1997, **40**(5), 1131–1143.
14. Yilbas, B. S., The validity of Fourier theory of radiation heating of metals. *Res. Mechanica*, 1988, **24,** 377–382.

15. Yilbas, B. S., Heating of metals at a free surface by laser irradiation—an electron kinetic theory approach. *International Journal of Engineering Science*, 1986, **24**(8), 1325–1334.
16. Qin, T. W. and Tien, C. L., Short pulse laser heating on metals. *International Journal of Heat and Mass Transfer*, 1992, **35**(3), 710–726.
17. Yilbas, B. S. and Sami, M., Laser heating mechanisms including evaporation process—semi classical and kinetic theory approaches. *Jpn. J. Appl. Phys.*, 1995, **34**, 6391–6400.
18. Mott, N. F. and Jones, H., *Theory of Properties of Melts and Alloys*. Dover Publ. London, 1978.
19. Brorson, S. D., Kazeroonkian, A., Moodera, J. S., Face, D. W., Cheng, T. K., Ippen, E. P., Dresselhaus, M. S. and Dresselhaus, G., Femtosecond room-temperature measurement of the electron–photon coupling constant λ in metallic superconductors. *Physical Review Letters*, 1990, **64**(18), 2172–2175.
20. Kittel, C. and Herbert, K., *Thermal Physics*, 2nd edn. W. H. Freeman, San Francisco, 1980.

APPENDIX

The energy equation after applying an explicit scheme may yield:

$$
\begin{aligned}
T(x,y,z,t+\mathrm{d}t) &= \frac{I_0^1 \Delta t}{2\sqrt{\pi}a\rho C_p} \\
&\times \exp\left[-\frac{y^2+z^2}{a^2}\right]\cdot\int_x^s \frac{N_{sx}}{N_{sx}+N_{xs}}\cdot f'(\psi)\,\mathrm{d}\psi \\
&+\frac{fk}{4\lambda^3}\frac{\Delta t}{\rho C_p}\left[\int_0^\infty \exp\left(-\frac{|x-s|}{\lambda}\right)\cdot T(s,y,z,t)\,\mathrm{d}s\right. \\
&+\int_0^x \exp\left(-\frac{|x-s|}{\lambda}\right)\cdot T(s,y,z,t)\,\mathrm{d}s \\
&\left.+\int_0^\infty \exp\left(-\frac{|x-s|}{\lambda}\right)\cdot T(s,y,z,t)\,\mathrm{d}s\right] \\
&+\frac{fk}{2\lambda^3}\frac{\Delta t}{\rho C_p}\left[\int_0^\infty \exp\left(-\frac{|y-\eta|}{\lambda}\right)\cdot T(x,\eta,z,t)\,\mathrm{d}\eta\right] \\
&+\frac{fk}{2\lambda^3}\frac{\Delta t}{\rho C_p}\left[\int_0^\infty \exp\left(-\frac{|z-\xi|}{\lambda}\right)\cdot(x,y,\xi,t)\right] \\
&+T(x,y,z,t)\left[1-\frac{3fk\Delta t}{2\lambda^2\rho C_p}-\frac{k}{2\mu^2}(p_{fm}h+p_{bm}g-2p_h)\right] \\
&+\frac{k\Delta t}{\rho C_p}\int_{-\infty}^\infty \frac{p_{fm}h}{2\mu^2}\exp\left(-\frac{|x-s|}{\mu}\right)T(s,y,z,t)\,\mathrm{d}s \\
&+\frac{k\Delta t}{\rho C_p}\int_{-\infty}^\infty \frac{p_{bm}g}{2\mu^2}\exp\left(-\frac{|x-s|}{\mu}\right)T(s,y,z,t)\,\mathrm{d}s \\
&+\frac{k\Delta t}{\rho C_p}\int_{-\infty}^\infty \frac{p_h}{2\mu^2}\exp\left(-\frac{|x-s|}{\mu}\right) \\
&\times[U(s)-U(x)+3k_B T(s,y,z,t)\,\mathrm{d}s\Big].
\end{aligned}
$$

Evaluation of the integrals

The integrals involved in the energy equation are computed using the trapezoidal method. According to this method, a function f is computed from an initial point 1 to a final point n using the values of f at equally spaced discrete points, i.e.:

$$\text{Integral} = \frac{h}{2}[f_1+2f^2+2f^3+\cdots+f_n]$$

where $f_1, f_2, \ldots, f_n$ are the values of the function at points 1, $2, \ldots, n$ and h is the spatial increment between successive points. Hence if the integrals are denoted by

$$G_1 = \int_0^\infty \exp\left(-\frac{|x-s|}{\lambda}\right)\cdot T(s,y,z,t)\cdot \mathrm{d}s$$

$$G_2 = \int_0^x \exp\left(-\frac{|x-s|}{\lambda}\right)\cdot T(s,y,z,t)\cdot \mathrm{d}s$$

$$G_3 = \int_x^\infty \exp\left(-\frac{|x-s|}{\lambda}\right)\cdot T(s,y,z,t)\cdot \mathrm{d}s$$

$$G_4 = \int_0^\infty \exp\left(-\frac{|y-\eta|}{\lambda}\right)\cdot T(s,y,z,t)\cdot \mathrm{d}\eta$$

$$G_5 = \int_0^\infty \exp\left(-\frac{|x-\xi|}{\lambda}\right)\cdot T(s,y,\xi,t)\cdot \mathrm{d}\xi$$

$$G_6 = 2\int_0^\infty \frac{p_{fm}h}{2\mu^2}\exp\left(-\frac{|x-s|}{\mu}\right)\cdot T(s,y,z,t)\cdot \mathrm{d}s$$

$$G_7 = 2\int_0^\infty \frac{p_{bm}g}{2\mu^2}\exp\left(-\frac{|x-s|}{\mu}\right)\cdot T(s,y,z,t)\cdot \mathrm{d}s$$

$$G_8 = 2\int_0^\infty \frac{p_h}{2\mu^2}\exp\left(-\frac{|x-s|}{\mu}\right)\cdot k_B T(s,y,z,t)\cdot \mathrm{d}s$$

then the approximation to one of these integrals, G_1 can be written as

$$
\begin{aligned}
G_1 = \int_0^\infty \frac{\Delta x}{2}\Bigg[&\exp\left(-\frac{|x+s_0|}{\lambda}\right)\cdot T(s_0,y,z,t) \\
&+2\exp\left(-\frac{|x+s_1|}{\lambda}\right)\cdot T(s_1,y,z,t)+\cdots \\
&+\exp\left(-\frac{|x+s_{n-1}|}{\lambda}\right)\cdot T(s_{n-1},y,z,t) \\
&+\exp\left(-\frac{|x+s_n|}{\lambda}\right)\cdot T(s_n,y,z,t)\Bigg]
\end{aligned}
$$

where

$$
\begin{aligned}
s_1 &= \Delta x \\
s_2 &= 2\Delta x \\
&\vdots\ \ \vdots \\
s_n &= n\Delta x
\end{aligned}
$$

where Δx is the spatial increment. The expressions for G_2–G_8 also involve the exponentials, so in order to generalize, the exponential terms are defined as:

$$A_7(j,m) = \sum_{j=1}^{n+1}\sum_{m=1}^{n+1}\exp\left(-\frac{|j\Delta x - m\Delta x|}{\lambda}\right)$$

$$A_8(j,m) = \sum_{j=1}^{n+1}\sum_{m=1}^{n+1}\exp\left(-\frac{|j\Delta x - m\Delta x|}{\lambda}\right)$$

$$A_{81}(j,m) = \sum_{j=1}^{n+1}\sum_{m=1}^{n+1}\exp\left(-\frac{|j\Delta y - m\Delta y|}{\mu}\right)\cdot$$

$$A_{82}(j,m)=\sum_{j=1}^{n+1}\sum_{m=1}^{n+1}\exp\left(-\frac{|j\Delta x-m\Delta x|}{\mu}\right)$$

$$A_{91}(j,m)=\sum_{j=1}^{n+1}\sum_{m=1}^{n+1}\exp\left(-\frac{|j\Delta x-m\Delta x|}{\mu}\right)\cdot\frac{p_{\mathrm{fm}}\cdot h}{2\mu^2}$$

$$A_{92}(j,m)=\sum_{j=1}^{n+1}\sum_{m=1}^{n+1}\exp\left(-\frac{|j\Delta x-m\Delta x|}{\mu}\right)\cdot\frac{p_{\mathrm{bm}}\cdot g}{2\mu^2}$$

and

$$A_{93}(j,m)=\sum_{j=1}^{n+1}\sum_{m=1}^{n+1}\exp\left(-\frac{|j\Delta x-m\Delta x|}{\mu}\right)\cdot\frac{p_{\mathrm{h}}}{2\mu^2}.$$

Therefore, the integrals yield in a final form:

$$G_1=\frac{\Delta x}{2}\left[A_8(j,1)\cdot T(1,y,z,t)+2\sum_{r=2}^{n}A_8(j,r)\cdot T(r,y,z,t)+A_8(j,n+1)\cdot T(n+1,y,z,t)\right]$$

$$G_2=\frac{\Delta x}{2}\left[A_7(j,1)\cdot T(1,y,z,t)+2\sum_{r=1}^{n}A_7(j,r)\cdot T(r,y,z,t)+A_7(j,j)\cdot T(j,y,z,t)\right]$$

$$G_3=\frac{\Delta x}{2}\left[A_7(j,j)\cdot T(j,y,z,t)+2\sum_{r=j+1}^{n}A_7(j,r)\cdot T(r,y,z,t)+A_7(j,n+1)\cdot T(n+1,y,z,t)\right]$$

$$G_4=\frac{\Delta y}{2}\left[A_{81}(j,1)\cdot T(x,1,z,t)+2\sum_{r=2}^{n}A_{81}(j,r)\cdot T(r,y,z,t)+A_{81}(j,n+1)\cdot T(x,n+1,z,t)\right]$$

$$G_5=\frac{\Delta z}{2}\left[A_{82}(j,1)\cdot T(x,y,1,t)+2\sum_{r=2}^{n}A_{82}(j,r)\cdot T(r,y,z,t)+A_{82}(j,n+1)\cdot T(x,y,n+1,t)\right]$$

$$G_6=\frac{\Delta z}{2}\left[A_{91}(j,m)\cdot T(j,y,z,t)+2\sum_{r=j+1}^{n}A_{91}(j,r)\cdot T(r,y,z,t)+A_{91}(j,n+1)\cdot T(n+1,y,z,t)\right]$$

$$G_7=\frac{\Delta z}{2}\left[A_{92}(j,m)\cdot T(j,y,z,t)+2\sum_{r=j+1}^{n}A_{92}(j,r)\cdot T(r,y,z,t)+A_{92}(j,n+1)\cdot T(n+1,y,z,t)\right]$$

$$G_9=\frac{\Delta z}{2}\left[A_{93}(j,m)\cdot T(j,y,z,t)+2\sum_{r=j+1}^{n}A_{93}(j,r)\cdot T(r,y,z,t)+A_{93}(j,n+1)\cdot T(n+1,y,z,t)\right].$$

As can be observed, the explicit representation gives the future temperature at $(x,y,z,t+\mathrm{d}t)$ in terms of the current temperatures at (x,y,z,t) and its surroundings nodes. Hence, knowing only the initial temperatures for all the nodes, the individual nodal temperatures for the next time step can be calculated. However, the explicit formulation faces the problem of stability, and careful choice of the time increment is required. The upper limit of the allowable time increment is given by

$$\frac{3fk\Delta t}{2\lambda^2\rho C_{\mathrm{p}}}\leqslant 1$$

so the second term of the right-hand side of the energy equation remains positive. If we let

$$A=\frac{I_0^1\Delta t}{2\sqrt{\pi}a\rho C_{\mathrm{p}}}\exp\left[-\frac{y^2+z^2}{a^2}\right]$$

$$B=\left[1-\frac{3fk\Delta t}{2\lambda^2\rho C_{\mathrm{p}}}-\frac{k}{2\mu^2}(p_{\mathrm{fm}}h+p_{\mathrm{bm}}g+2p_{\mathrm{h}})\right]$$

$$C=\frac{f\cdot k\Delta t}{4\lambda^3\rho C_{\mathrm{p}}}$$

$$D=\frac{k\Delta t}{\rho C_{\mathrm{p}}}$$

and G_1–G_5 are as defined above, then equation (4) can be written as

$$\bar{T}(x,t+\Delta t)=A\cdot(\delta x)+B\cdot\bar{T}(x,t)+C\cdot(G_1+G_2+G_3+2G_4+2G_5)+D(2G_5+2G_6+2G_7+2G_8)$$

and from there we obtain the stability criterion as

$$B\geqslant 0.$$

A computer program has been developed to solve the energy equation.